Topslam: Waddington Landscape Recovery for Single Cell Experiments

Max Zwiessele[1,*], Neil D Lawrence[1],

1 University of Sheffield, Department of Computerscience

* m.zwiessele@sheffield.ac.uk

Abstract

We present an approach to estimating the nature of the Waddington (or epigenetic) landscape that underlies a population of individual cells. Through exploiting high resolution single cell transcription experiments we show that cells can be located on a landscape that reflects their differentiated nature.

Our approach makes use of probabilistic non-linear dimensionality reduction that respects the topology of our estimated epigenetic landscape. In simulation studies and analyses of real data we show that the approach, known as topslam, outperforms previous attempts to understand the differentiation landscape.

Hereby, the novelty of our approach lies in the correction of distances *before* extracting ordering information. This gives the advantage over other attempts, which have to correct for extracted time lines by post processing or additional data.

High-throughput single-cell real-time polymerase chain reaction gene expression measurements (Section S2) are new and promising techniques to give insights into the heterogeneous development of individual cells in organism tissues [19]. However, interpretation of measurements can be highly challenging.

Waddington [32, 33] proposed an analogy for understanding the process of differentiation, known as Waddington's landscape or the *epigenetic landscape*. The analogy is based around the idea that differentiated cells are located at different points on the epigenetic landscape with particular paths through the landscape more likely than others due to its underlying topology. Think of a map of an alpine area, historically populations became isolated in valleys and differentiated. Topology and location are key aspects of the analogy.

Visualisation of such landscapes is an important aid to biologists involved in studying the evolution of individual cells either in development or cancer. In this paper we reconstruct such landscapes from rich phenotype information from each of the individual cells. In particular, we extract maps of the epigenetic landscape given the observations of *gene expression*.

The mathematical underpinnings of mapping involve a projection from a low dimensional space to a higher dimensional space. Classically we might wish to project the three dimensional world around us down to two dimensions for use as a map or a chart. Formally this involves a mapping, $\mathbf{f}(\cdot)$ from the positions in the two dimensional space, $\mathbf{x}$, to our measurements, $\mathbf{y}$:

$$\mathbf{y} = \mathbf{f}(\mathbf{x}).$$

In epigenetic landscapes, rather than considering the high dimensional measurements to be direct measurements of the physical world around us, we instead observe a rich phenotype, such as the gene expression of an individual cell, $\mathbf{y}$. Our aim is to develop a coherent map such that the position of each cell, $\mathbf{x}$, is consistent with cells that are

expressing a similar phenotype. In other words, if two cells have a similar gene expression they should be located near to each other in the map, just as two people located near to each other in a real landscape would have a similar view.

The utility of a map is given by the precision in which it can be recreated. Geographic surveys were originally created through triangulation and laborious ground level surveys. The challenges we face for the epigenetic landscape are somewhat greater. In particular the measurements of phenotype are subject to a great deal of noise, particularly in single cell experiments, in other words there is a mistiness to the observations. Further, we cannot access all areas. We can only query individual cells as to their particular phenotype, we cannot move around the landscape at will. Finally, there is a complex, most likely non-linear relationship between any location on the map which is unknown.

We are inspired by challenges in robotics: in robot navigation a robot facing a landscape for the first time needs to continually assess its current position (the values of $\mathbf{x}$) and simultaneously update its estimate of the map (the function $f(\cdot)$). This challenge is known as as simultaneous localisation and mapping (SLAM [26]).

For example Ferris *et al.* [9] showed how simultaneous localisation and mapping could be formed by measuring the relative strength of different WiFi access points as it moves around a building. When you are near to a given access point you will receive a strong signal, when far, a weak signal. If two robots both perceive a particular access point to have a strong signal they are likely to be near each other. We can think of the WiFi access points as landmarks. In our case landmarks are the (noisy) gene expression measurements. If two cells have a similar set of gene expression measurements they are also likely to be near each other. A further challenge for our algorithm is that gene expression measurements are very high dimensional and can be extremely noisy. Because of the analogy to SLAM algorithms and our use of topology to develop the landscape we refer to our approach as *topslam* (topologically aware simultaneous localisation and mapping).

The relationship between the epigenetic landscape and the observed data is dependent on a complex set of interactions between transcription factors, genes and epigenomic modifications. Unpicking the mechanism behind this relationship is extremely challenging [2]. Instead we propose an alternative, data driven approach based on machine learning algorithms and judicious application of probabilistic methods.

Quantitative determination of single-cell gene expression is commonly used to determine the—known to be heterogeneous—differentiation process of cells in cancer [7] or in the early development of multicell organisms [14]. The measurement of single cells, however, can give rise to systematically introduced errors in the identification of sub processes in the cell and in the assignment of cells to their specific cell-lines. This is due to the low amounts of mRNA available in single cells: the mRNA requires amplification using polymerase chain reaction (PCR, see e.g. [11, 16, 20]).

These technical limitations complicate analysis: they introduce non-linear effects and systematic errors. So as promising as high throughput methods are, they require sophisticated analyses to resolve confounding factors. By providing the scientist with the underlying Waddington landscape for cells in a given experiment, along with the location of each cell in the landscape, we hope to significantly simplify this process. Unpicking the nature of the genetic landmarks in the presence of noise typically exploits *feature extraction*, where high dimensional gene expression data has its dimensionality reduced [10, 14, 22, 23], often through linear techniques. However, it is difficult to determine the number of dimensions to use for further analyses [3–5].

1.1 Dimensionality Reduction

Dimensionality reduction gives a view on the landscape of the underlying biological system. To perform dimensionality reduction we need a mathematical model that extracts the salient aspects of the data without exhibiting vulnerability to confounding factors such as technical or biological noise.

Probabilistic models aim to trade off the useful structure with the confounding variation through specifying probability distributions for each component. We consider non-linear probabilistic models that not only model the landscape as a non-linear surface (think of an irregular skiing piste, in which you want to turn into the flat bits, as opposed to a flat beginners slope, where you can just go in a straight line), but also allow us to determine the dimensionality necessary to explain the gene expression variation, while explaining away the noise through a separate model component.

Linear methods can also be given probabilistic underpinnings, but they suffer from the severe constraint of only allowing the landscape to be linearly related to the genetic landmarks. Conversely deterministic (i.e. non-probabilistic) non-linear methods do not offer a principled approach to separating the confounding variation from the landscape's underlying structure. It can be hard to grasp topographical relationships due to the deterministic nature of the technique. Either additional data or additional correctional deterministic algorithms are necessary for a coherent mapping [1, 24].

We make use of the Bayesian Gaussian process latent variable model (Bayesian GPLVM [28]), a probabilistic dimensionality reduction technique that extracts the relevant dimensionality of the latent embedding as well as expressing a non-linear model. Further, we make use of the *geometry* of the underlying map by exploiting recent advances in metrics for *probabilistic* geometries [29].

1.2 PCA and Graph Maps

An approach such as principal component analysis (PCA) makes an assumption of a *linear* relationship between the high dimensional measurements and the cell's location in the landscape. This limiting assumption is normally alleviated by proceeding in a two step manner. First PCA is done for all data, then the locations in the linear map are clustered and a further PCA is applied to each cluster separately, giving one coordinate system per cluster [14] (see also [27] for an elegant implementation of this approach).

Islam *et al.* [18] developed a graph based method, using similarities of cell profiles to characterise two different cell types in a so called "graph map".

The underlying probabilistic dimensionality reduction technique has been successfully used in other applications to single cell transcriptomics data, e.g. for visualisation [3], to uncover sub populations of cells [4] and to uncover transcriptional networks in blood stem cells [21].

Our topslam approach is a generalisation of the idea of "graph maps": Waddington's landscape [32, 33] can be seen as a non-linear map for the branching process of cells, where the cell process is described as a ball rolling down a hill following stochastically (by e.g. cell stage distribution) the valleys of the hillside (Fig. 1).

The novelty of our approach is to not correct *after* extraction of graph information, but to correct the distance the graph extraction *uses to extract* information. We can do that by estimating the underlying Waddington landscape along differentiation of cells.

1.3 Independent Component Analysis and Non-linear Dimensionality Reduction

Recovery of the epigenetic landscape as an intermediate step facilitates the extraction of other characteristics of interest, such as pseudotime, in cell stage development. For
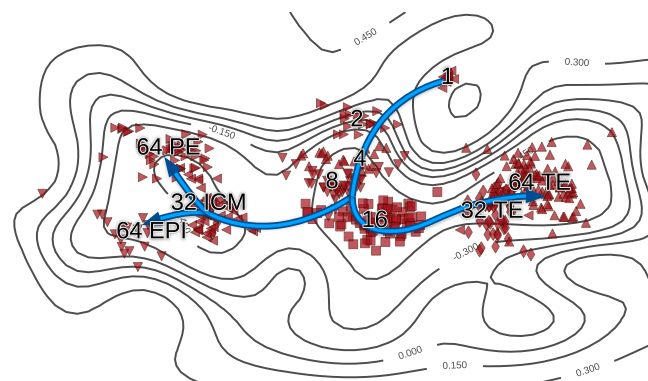
Figure 1. Representation of the probabilistic Waddington's landscape. The contour lines represent heights of the landscape. We want to be in the valleys of this landscape (akin valleys of mountains). The time is then extracted along the cells such that it follows the landscape, depicted as splitting arrows. This also reflects the separate cell fates in the epigenetic progression of the cells.

example Trapnell *et al.* [30] apply independent component analysis (ICA, see e.g. [17]) on the gene expression experiment matrix to develop a low dimensional representation of the processes. They then build a minimal spanning tree (MST) on the distances developed from the resulting latent representation to reconstruct a Waddington's landscape given by ICA. After some correction, if there are branching processes, they report the longest paths along the MST as the pseudotime backbone and the summed distances as the pseudotime ordering for each cell. However, this method relies on having rough estimates of the capture time to induce the ordering in the pseudotime estimate. Our probabilistic description of Waddington's landscape relieves this requirement and allows for post analysis of data sets which do not provide such estimates.

Other methods apply deterministic non-linear dimensionality reductions and attempt to recover the underlying pseudotime in a probabilistic framework [6]. The Wanderlust algorithm applies the t-SNE [31] algorithm to reduce the dimensionality of the expression matrix and then proceeds by averaging over k-nearest-neighbour graph ensembles to extract pseudotimes.

Usually now other methods employ heuristics or additional data about capture times to correct for distances in the extracted landscape. For this, they rely on euclidean distances between cells to overlay the extraction method of pseudo time (usually graphs, on which to go along). For us, we can employ non euclidean distances in the landscape, following the topography of the probabilistic landscape to use in the graph, which can correct for outliers, which will be identified by the landscape's topography.

A Riemannian geometry distorts distances, just as in a real map movement is not equally easy in all directions (it is easier to go down hill or follow roads) the underlying Waddington landscape has a topology which should be respected. Topslam landscapes are both non-linear and probabilistic and we correct, locally, for Riemannian distortions introduced by the non-linear surfaces. In the next section we will show how the combination of these three characteristics allows us to recover pseudotime *without* reliance on additional data or additional (correctional) algorithms for graph extraction, to correct for the underlying dimensionality reduction technique used.

In summary we introduce a probabilistic approach to inferring Waddington landscapes and we consider the topological constraints of that landscape. In the next
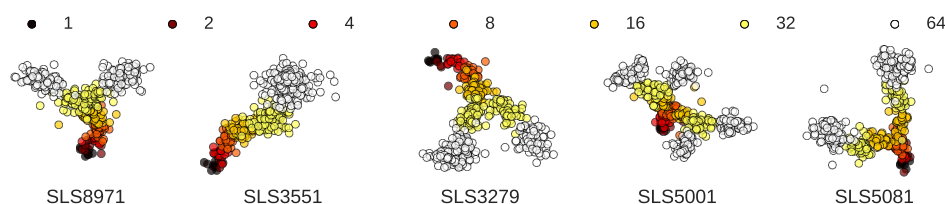
Figure 2. Simulated differentiation processes along cell stages. The cell stages are coloured from 1 to 64 cell stage and each simulation has its associated unique seed printed underneath. The selection of differentiation processes was done by visual inspection, strafing for variety and non overlapping profiles, so that a 2 dimensional landscape was possible.

section we show how this idea can be used to improve pseudotime recovery for single cell data.

2 Application: Pseudotime Recovery

Single cell gene expression experiments provide unprecedented access to the underlying processes and intrinsic functional relationships of and between cells. However, looking at single cells the extracted gene expression is prone to the heterogeneous variability from cell-to-cell. Such noise is not only technical (such as low amounts of RNA, dropout events etc. [19]), but also biological in origin (heterogeneity between cells of the same type).

Each cell is a functioning member of a local community of cells. Biology is based on an evolutionary progression, in which old systems are usually kept in place, when new ones are found. This introduces a lot of redundancies in such processes and makes extraction of information and evidence complex. Therefore, we use dimensionality reduction techniques to optimise and visualise the underlying landscape of the biological process.

Epigenetic progression is a discrete process that Waddington suggested could be visualised as part of a continuous landscape. However, the relationship between location on the landscape and the measured state of the cell is unlikely to be *linear*.

Further, when mapping natural landscapes, a laborious process of triangulation through high precision measurements is used to specify the map accurately. In the epigenetic landscape, no such precision is available. As a result it is vital that we sustain an estimate of our *uncertainty* about the nature of the landscape as we develop the map.

2.1 Simulation and Validation

Simulation was done by simulating 5 differentiation patterns of cells (Fig. 2). We then extracted pseudotime orderings of the cells in the simulation from 10 repetitions of creating gene expression measurements driven by the simulated differentiation patters (details Supplementary S1).

2.1.1 Simulation Results

We compare extracted pseudotime orderings of all three methods in Figure 3. Plotted are the linear regression correlation coefficients ρ between simulated and extracted time lines. From the simulation studies we can extract, that we can fully reconstruct the simulated time at an average correlation of approximately 91%[±4%] (Table 1). This is
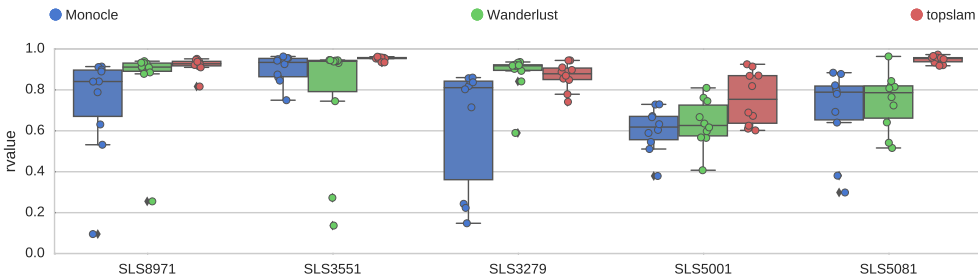
Figure 3. Simulation study results for gene expression matrices generated from simulated Waddington landscapes along a time line. Shown are linear regression Pearson correlation coefficients ρ between extracted and simulated time lines. Data sets where simulated from different differentiation profiles as described in Section S1.

more then 10% higher correlation then the next best method Wanderlust (at 78%[±18%]). The construction of Waddington's landscape ensures an improvement over the other methods in all simulated latent spaces, even if the intrinsic signal structure suits the other methods. Additionally, the consistency of our result is higher across the experiments, providing more reliable results over multiple experiments.

The simulation results show, that topslam is robust to repetition and differences in underlying surfaces, whereas the other methods fail in certain circumstances, especially when the underlying differentiation process gets complex (more branching). Thus, it is crucial to account for the topography of the dimensionality reduction technique, before extracting intrinsic signals (such as pseudotime) from the rich phenotypic characterisations of cells.

We also show, that we can use topslam to overlay a probabilistic Waddington's landscape over the other dimensionality reduction techniques. This enables a corrected extraction of pseudotime estimates. This correction is shown to be never detrimental and can increase the correlation between extracted and simulated pseudotimes (Supplementary S1). The supplementary material also contains results for a range of other dimensionality reduction techniques.

2.1.2 Running Time

Our probabilistic treatment of landscape recovery and our principled correction of the topology mean that topslam is the slowest of the three approaches. The other two methods only apply heuristic corrections, gaining speed in the estimation of intrinsic signal ordering. Topslam averages at approximately $230s$ of run time to learn the landscape for the simulated $400 - 500$ cells. (The number of genes does not play a significant role during optimisation, because of pre-computation of the empirical covariance matrix.) Wanderlust averages at approximately $40s$ and Monocle at only $5s$. However, as we've seen this faster compute comes at the expense of a significant loss of both accuracy and consistency. We now turn to deployment of topslam on real data.

3 Pseudotime Extraction for Human and Mouse Cells

In this section we explore the performance of topslam on to real single cell qPCR (Supplementary S2.1) and single cell RNA-seq (Supplementary S2.2) experiments. This shows the ability for topslam to extract intrinsic signals for existing and difficult single
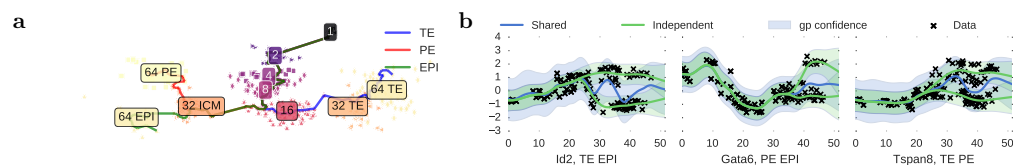
Figure 4. a Differentiation process along the time graph (endpoints randomly chosen within respective cell type). These differentiation paths are used for differential gene expression for marker gene detection. **b** Some example plots for the marker genes. In green you can see the individual fits of two GPs, sharing one prior, and in blue the shared fit of one GP to all the data. Differential expression is decided on which of those two models (green or blue) fits the data better. Note the time line elucidates when (in time) the gene can be used as a marker gene. *Gata6* is a known marker for TE, but evidently it is also differentially expressed in mice between PE and EPI differentiation states.

cell profiling techniques, which can bare difficulties because of high noise corruption and systematic errors (dropouts, detection limit etc.). 227, 228

3.1 Mouse Embryonic Development Landscape

We extract the pseudotime for a mouse embryonic single cell qPCR experiment [13,19] of 437 cells, captured from one to 64 cell-state. In this experiment 48 genes where captured. We learn a landscape for the cells progression along time, capturing the differentiation process. The landscape then defines the progression of time by following the valleys of the topography, depicted in Figure 1.

Extracting the progression landscape from a qPCR single cell gene expression experiment [14] reveals the time line for the single cell progression in fine grained detail. We extract the landscape for the developmental cells and compute distances along the landscape through an embedded graph.

The starting cell needs to be given, whereas no more information is needed to extract the progression of (pseudo-) time along the graph. It is recommended to provide a leaf node in the graph, to ensure only one direction of time along Waddington's landscape. We can now use the extracted time to infer differing progression of gene expression through the progression of cells. In this particular data set we have a differentiation progress at hand, cells differentiating into three different cell states in the 64 cell stage: trophectoderm (TE), epiblast (EPI), and primitive endoderm (PE).

We use the same labelling of Guo *et al.* [14], which introduces some systematic errors (as explained in Section 1.1). With this differentiation, we can now plot gene expression along the landscape, revealing the dynamics of gene expression during differentiation and elucidating differentiation processes within different cell types (Fig. 4). Using the extracted pseudotime for different pathways in the cell stages, we can elucidate the differentiation process along time. We perform differential gene expression detection in time series experiments (e.g. [25]), and use the top ten differentially expressed genes as marker genes for the three cell stages (Table 2). We compiled the list as a comparison between stages, thus if a gene is duplicated in the comparison of stages it is a marker gene for the differentiation of the one stage from the two others (see e.g. for TE *Id2*, *Tspan8*). The differentiation takes place in the 16 and 32 cell stages (Figure 4). Having the time series as differential expressed marker genes, we can plot the exact time line of when genes get differentially expressed along pseudo time (Figure 4).

Comparison with results using other dimensionality reduction techniques, show that the other methods are not able to capture the non-linearities in the data (topslam is our method, Figure 5). We can also see the representation of Waddington's landscape as
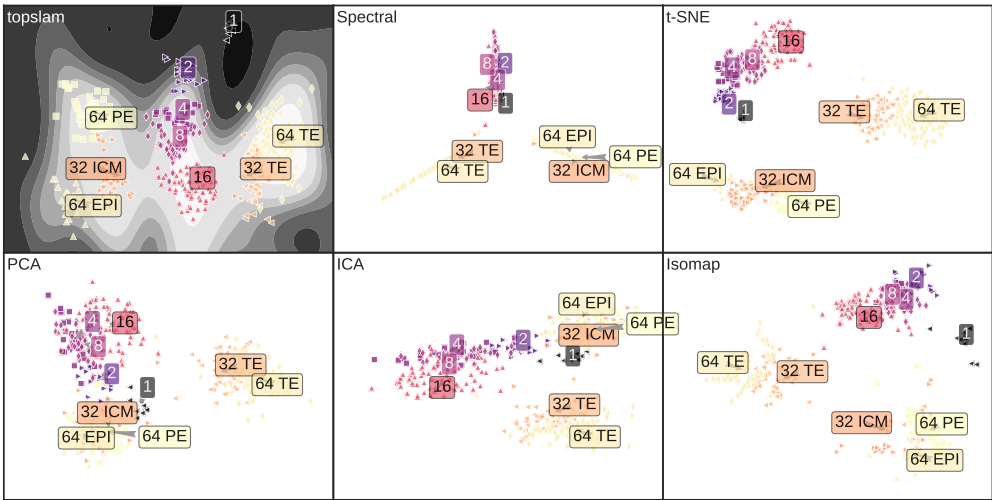
Figure 5. Comparison plots between different dimensionality reduction techniques for the Guo *et al.* data set of developmental mouse embryonic stem cells [14]. As can be seen, only topslam (probabilistic Waddington landscape) can fully identify the relationships between the cells and order them correctly for pseudo time extraction. t-SNE is the underlying method Wanderlust relies on and ICA the one for Monocle.

shaded area, we want to stay in light areas.

Using the probabilistic interpretation of Waddington's landscape as a correction for the embedding and extraction techniques, we can extract pseudotime information more clearly and without additional information to ensure the time line extracted corresponds to the cell stages as seen in Guo *et al.* [14].

3.2 Monoallelic Mouse Embryonic Landscape

Deng *et al.* [8] perform an exploratory single cell RNA-seq experiment for allele specific gene expression. They find significant differences between paternal and maternal developmental development in split-cell experiments (see [8] for details). Performing a PCA on the extracted Gene Expression Experiment reveals the overall time structure from oocyte to blastocyst. However, PCA fails to recover the differences in monoallelic expression (See PCA in Figure 6).

Generating a probabilistic Waddington's landscape for this experiment not only reveals the dynamics of overall pre-implantation development, but also it enables us to distinguish between split-cells and others (Fig. 7). Suggestively there may also be a closer relationship between the split-cells and adult cells, although given that similarity with early development cells is unlikely to be great, that conclusion should be treated with some caution.

Again, the probabilistic representation of Waddington's landscape reveals a detailed description of the cells developmental progression. It picks out sub populations in the cells, which were not visible by other dimensionality reduction techniques (Figure 7).

3.3 Human Developmental Landscape

In this experiment Yan *et al.* [34] looked for connections between human embryonic stem cell gene expression and pre-implantation embryo gene expression. We use the data set to show the embryonic developmental landscape in humans, by extracting the
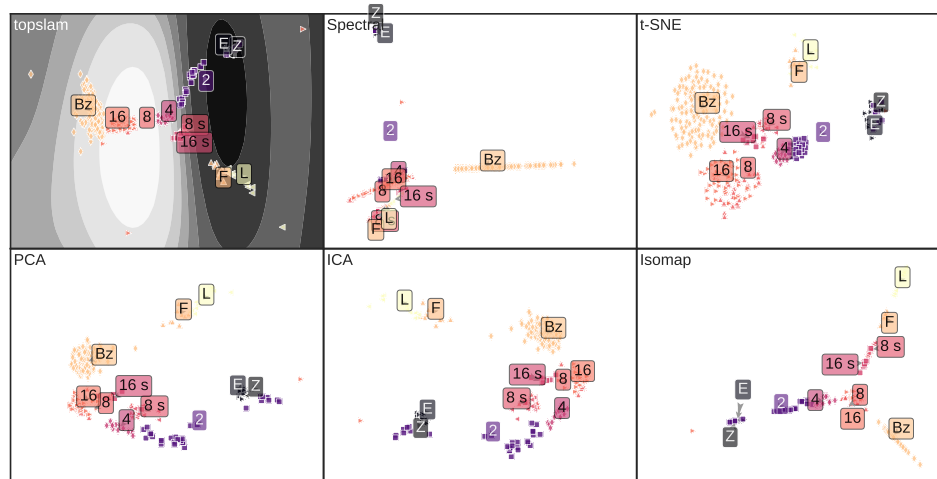
Figure 6. Comparing different dimensionality reduction techniques applied to the pre-implantation developmental gene expression experiment from Deng *et al.* [8]. Again, you can see that the other methods struggle to reveal the underlying structure of the experiment. A split-cell experiment was performed, depicted with an 's' attached to the label (8s and 16s). Additionally, fibroblasts (F) and liver cells (L) where measured and are included in the time line here.
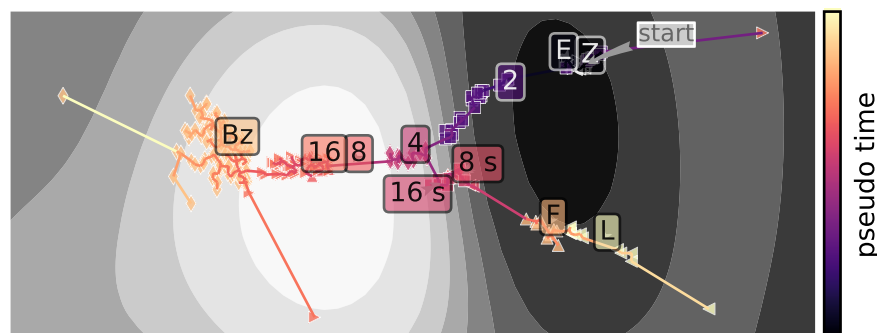

Figure 7. The pseudo time extracted by the probabilistic handling of Waddington's landscape from monoallelic embryonic stem cells from oocyte to blastocyst. A split-cell experiment was performed, depicted with an 's' attached to the label (8s and 16s). Additionally, fibroblasts (F) and liver cells (L) where measured and are included in the time line here. They appear to be closer to the split-cells, though this could be an artefact of the huge time line difference between cells. The shading shows Waddington's landscape as grey scales, from dark (un-favoured) to light (favoured).
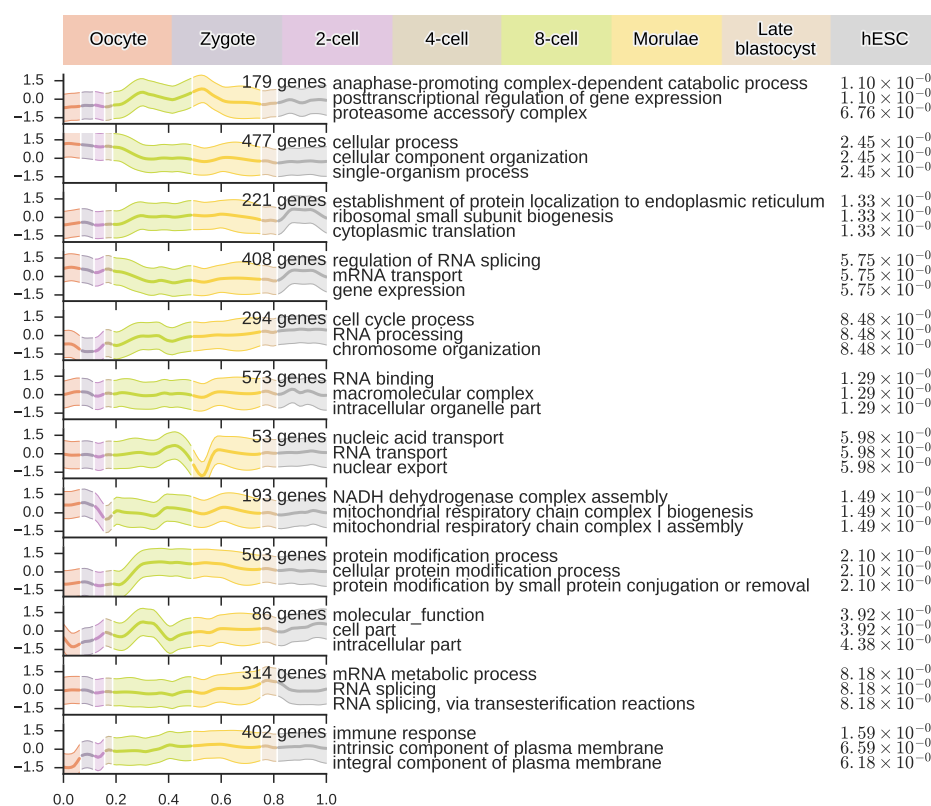
Figure 8. Clusters extracted using Hensman *et al.* [15] from human embryonic stem cell gene expression. The number of genes matching the clusters is shown in the north east of each subplot. Each subplot shows one cluster mean (thick line) and variance (shaded area). Here the genes are all genes, fully observed in the data set. In the top we see the colouring for the cell stages along the time line. The right shows the top 3 gene ontology associations and their Benjamini-Hochberg corrected *p*-values.

probabilistic representation of Waddington's landscape of the one cell state, through the late blastocyst stage to human Embryonic Stem Cells (hESC).

Again, comparing our representation to other dimensionality reduction techniques (Fig. S11) reveals the ability of the probabilistic modelling to capture the underlying time structure of the cells. (Heavy filtering was done to select only highly variable genes, this removed the very large number of dropout events and low expressed genes (See supplementary material S4.2,S1).)

We extract the landscape and pseudotimes along the graph (Fig. S10). This enables us to consider other analyses such as time-series clustering [15]. Such studies could further unravel processes on a genetic level.[1] To validate the clusters we performed a gene ontology association study shown on the right of the cluster distributions (Fig. 8). These clusters are referring to the hESC cells as a follow up stage after the late blastocyst, as the topography of the Waddington landscape suggests.

The gene ontology associations show that the hESC cell stage genes are up regulated towards ribosomal activity and RNA activity. Genes up regulated towards the end of the pre-implantation cell stages (late blastocyst) are associated with RNA splicing and mRNA metabolic processes. We used the goatools toolbox to perform the gene ontology analysis [34]. With topslam we are able to resemble results found in Yan *et al.* [34],

---

[1]This clustering is performed on the non-filtered genes.

	SLS8971	SLS3551	SLS3279	SLS5001	SLS5081
Monocle	0.73±0.26	0.90±0.07	0.63±0.30	0.61±0.11	0.70±0.20
Wanderlust	**0.92**±0.01	0.91±0.05	0.84±0.14	0.65±0.10	0.60±0.21
topslam	**0.92**±0.02	**0.93**±0.01	**0.85**±0.03	**0.91**±0.03	**0.94**±0.01

Table 1. Simulation results for extracting pseudotime orderings using Monocle, Wanderlust and topslam. Results are shown as mean and standard deviation of Pearson correlation coefficient ρ between estimated and simulated times for all 5 simulations and over 10 repetitions.

TE EPI	PE EPI	TE PE
Id2	Fgf4	Pdgfra
Fgf4	Runx1	Id2
Bmp4	Fgfr2	Gata4
Pecam1	Gata6	DppaI
Sox2	Pdgfra	Tspan8
DppaI	Klf2	Atp12a
Fn1	Bmp4	Pecam1
Klf4	Gata4	Fn1
Fgfr2	Nanog	Creb312
Tspan8	Sox2	Runx1

Table 2. Marker genes for differentiation between the tree cell stages compiled from time series differential expression along the pseudotime. Shown are the ten most differentially expressed genes, pairwise between the three stages. For example *Id2* is differentially expressed between (TE and EPI) and between (TE and PE). This means it is a marker gene for TE, as it behaves differently from the two other differentiation stages, but not within the two others. *Id2* is known to be a marker for TE.

without the need for additional statistical filtering, such as anova or mean analysis. We are able to directly model the connection between time and genes employing probabilistic correction and modelling. This gives the advantage of providing more power, as more data points can be employed in the analysis.

Using topslam allows us to extract an actual time line along which we can do further studies. We do not have to employ binning procedures, which can introduce systematic errors and reduce statistical power.

4 Conclusion

We have introduced a probabilistic approach to inferring Waddington landscapes. We use rich phenotype information to characterise the landscape and probabilistic inference techniques to infer a non-linear mapping from the landscape to the phenotype. Our approach allows us to respect the topology of the landscape when extracting distances and we show the advantages of this idea when reconstructing pseudotimes from single cell data. Summarising single cells in this manner represents a powerful approach for understanding the evolution of their genetic profile, a critical stage in understanding development and cancer.

5   Methods

5.1   Data

For description of single cell transcriptome extraction techniques please refer to supplementary material S2.

5.2   Code

A package topslam written in python (based on GPy [12]) is provided for users to apply the methods described in this work.

    https://github.com/mzwiessele/topslam

We supply all topslam correction methods in this package, including different graph extraction techniques. Additionally, we supply optimisation routines for the dimensionality reduction technique. For you convenience we include plotting routines and data filtering methods alongside the package.

5.3   Extracting Pseudotime

The most common way of extracting pseudotime orderings is done with the following stages:

1. Extract lower dimensional representation $\mathbf{X} \in \mathbb{R}^{n \times q}$ of gene expression matrix $\mathbf{Y} \in \mathbb{R}^{n \times d}$ with n samples as rows and d genes as columns. The lower dimensional representation is often chosen to have $q = 2$ dimensions, as the dimensionality reduction techniques do not express a selection criterion and two dimensions are convenient for visualisation.

2. Supply starting point $\mathbf{s} \in \mathbf{X}$ of pseudotime ordering extracted in the next step.

3. Extract distance information about cells by following the landscape by a graph structure, sometimes a tree, or k-nearest-neighbour graph.

4. Extract the ordering of cells along the graph structure extracted in the above step (including smoothing, branch detection, and/or clustering).

5.3.1   Topslam Approach

Crucially standard approaches each miss at least one important component of the mapping problem. Monocle assumes a linear map, a highly unrealistic assumption. Wanderlust [1] makes use of a non-linear method but does not consider the *topography* of the map when developing pseudotime orderings. The topography of the epigenetic landscape influences distances between cells on the landscape, and therefore their effective relative positions to each other.

Our approach, a topologically corrected simultaneous localisation and mapping of cells, topslam, proposes to make use of a *probabilistic non-linear* dimensionality reduction technique, also used in many other single cell transcriptomics applications [3–5, 21]. The probabilistic nature of the dimensionality reduction technique is used for extracting the Waddington landscapes *with* associated uncertainties. Further, we are able to take account of the local topography when extracting pseudotimes, correcting distances by applying non euclidean metrics along the landscape [29].

To perform pseudotime extraction with topslam we build a minimum spanning tree (or k-nearest-neighbour graph) along the latent landscape uncovered by topslam. This allows the spanning tree to naturally follow the landscape topography and makes any corrections post extraction obsolete. For a more detailed description of the approach see supplementary material [S3,S4].

References

1. S. C. Bendall, K. L. Davis, E.-a. D. Amir, M. D. Tadmor, E. F. Simonds, T. J. Chen, D. K. Shenfeld, G. P. Nolan, and D. Pe'er. Single-cell trajectory detection uncovers progression and regulatory coordination in human B cell development. *Cell*, 157(3):714–725, 2014.

2. S. Bhattacharya, Q. Zhang, and M. E. Andersen. A deterministic map of Waddington's epigenetic landscape for cell fate specification. *BMC systems biology*, 5(1):85, 2011.

3. F. Buettner, V. Moignard, B. Göttgens, and F. J. Theis. Probabilistic PCA of censored data: accounting for uncertainties in the visualization of high-throughput single-cell qPCR data. *Bioinformatics*, 30(13):1867–1875, 2014.

4. F. Buettner, K. N. Natarajan, F. P. Casale, V. Proserpio, A. Scialdone, F. J. Theis, S. A. Teichmann, J. C. Marioni, and O. Stegle. Computational analysis of cell-to-cell heterogeneity in single-cell RNA-sequencing data reveals hidden subpopulations of cells. *Nature biotechnology*, 33(2):155–160, 2015.

5. F. Buettner and F. J. Theis. A novel approach for resolving differences in single-cell gene expression patterns from zygote to blastocyst. *Bioinformatics*, 28(18):i626–i632, 2012.

6. K. Campbell and C. Yau. Bayesian Gaussian Process Latent Variable Models for pseudotime inference in single-cell RNA-seq data. *bioRxiv*, page 026872, 2015.

7. P. Dalerba, T. Kalisky, D. Sahoo, P. S. Rajendran, M. E. Rothenberg, A. A. Leyrat, S. Sim, J. Okamoto, D. M. Johnston, D. Qian, et al. Single-cell dissection of transcriptional heterogeneity in human colon tumors. *Nature biotechnology*, 29(12):1120–1127, 2011.

8. Q. Deng, D. Ramsköld, B. Reinius, and R. Sandberg. Single-Cell RNA-Seq Reveals Dynamic, Random Monoallelic Gene Expression in Mammalian Cells. *Science*, 343(6167):193–196, 2014.

9. B. Ferris, D. Fox, and N. D. Lawrence. WiFi-SLAM Using Gaussian Process Latent Variable Models. In *IJCAI*, volume 7, pages 2480–2485, 2007.

10. R. A. Gibbs, J. W. Belmont, P. Hardenbol, T. D. Willis, F. Yu, H. Yang, L.-Y. Ch'ang, W. Huang, B. Liu, Y. Shen, et al. The international HapMap project. *Nature*, 426(6968):789–796, 2003.

11. A. Git, H. Dvinge, M. Salmon-Divon, M. Osborne, C. Kutter, J. Hadfield, P. Bertone, and C. Caldas. Systematic comparison of microarray profiling, real-time PCR, and next-generation sequencing technologies for measuring differential microRNA expression. *RNA*, 16(5):991–1006, May 2010.

12. GPy. GPy: A Gaussian process framework in python. http://github.com/SheffieldML/GPy, since 2012.

13. D. Grün and A. van Oudenaarden. Design and analysis of single-cell sequencing experiments. *Cell*, 163(4):799–810, 2015.

14. G. Guo, M. Huss, G. Q. Tong, C. Wang, L. Li Sun, N. D. Clarke, and P. Robson. Resolution of cell fate decisions revealed by single-cell gene expression analysis from zygote to blastocyst. *Developmental cell*, 18(4):675–685, 2010.

15. J. Hensman, M. Rattray, and N. D. Lawrence. Fast nonparametric clustering of structured time-series. *Pattern Analysis and Machine Intelligence, IEEE Transactions on*, 37(2):383–393, 2015.

16. D. S. Horner, G. Pavesi, T. Castrignanò, P. D. De Meo, S. Liuni, M. Sammeth, E. Picardi, and G. Pesole. Bioinformatics approaches for genomics and post genomics applications of next-generation sequencing. *Brief Bioinform*, 11(2):181–97, Mar 2010.

17. A. Hyvärinen, J. Karhunen, and E. Oja. *Independent component analysis*, volume 46. John Wiley & Sons, 2004.

18. S. Islam, U. Kjällquist, A. Moliner, P. Zajac, J.-B. Fan, P. Lönnerberg, and S. Linnarsson. Characterization of the single-cell transcriptional landscape by highly multiplex RNA-seq. *Genome research*, 21(7):1160–1167, 2011.

19. T. Kalisky and S. R. Quake. Single-cell genomics. *Nat Meth*, 8(4):311–314, Apr. 2011.

20. A. McDavid, G. Finak, P. K. Chattopadyay, M. Dominguez, L. Lamoreaux, S. S. Ma, M. Roederer, and R. Gottardo. Data exploration, quality control and testing in single-cell qPCR-based gene expression experiments. *Bioinformatics*, 29(4):461–467, 2013.

21. V. Moignard, I. C. Macaulay, G. Swiers, F. Buettner, J. Schütte, F. J. Calero-Nieto, S. Kinston, A. Joshi, R. Hannah, F. J. Theis, et al. Characterization of transcriptional networks in blood stem and progenitor cells using high-throughput single-cell gene expression analysis. *Nature cell biology*, 15(4):363–372, 2013.

22. P. Paschou, E. Ziv, E. G. Burchard, S. Choudhry, W. Rodriguez-Cintron, M. W. Mahoney, and P. Drineas. PCA-correlated SNPs for structure identification in worldwide human populations. *PLoS Genet*, 3(9):1672–86, Sep 2007.

23. C. Rampon, C. H. Jiang, H. Dong, Y.-P. Tang, D. J. Lockhart, P. G. Schultz, J. Z. Tsien, , and Y. Hu. Effects of environmental enrichment on gene expression in the brain. *PNAS*, November 2000.

24. M. Setty, M. D. Tadmor, S. Reich-Zeliger, O. Angel, T. M. Salame, P. Kathail, K. Choi, S. Bendall, N. Friedman, and D. Pe'er. Wishbone identifies bifurcating developmental trajectories from single-cell data. *Nature Biotechnology*, 2016.

25. O. Stegle, K. J. Denby, E. J. Cooke, D. L. Wild, Z. Ghahramani, and K. M. Borgwardt. A robust Bayesian two-sample test for detecting intervals of differential gene expression in microarray time series. *Journal of Computational Biology*, 17(3):355–367, 2010.

26. S. Thrun and J. J. Leonard. Simultaneous localization and mapping. In *Springer handbook of robotics*, pages 871–889. Springer, 2008.

27. M. E. Tipping and C. M. Bishop. Mixtures of probabilistic principal component analyzers. *Neural computation*, 11(2):443–482, 1999.

28. M. K. Titsias and N. D. Lawrence. Bayesian Gaussian Process Latent Variable Model. *Artificial Intelligence and Statistics*, 2010.

29. A. Tosi, S. Hauberg, A. Vellido, and N. D. Lawrence. Metrics for probabilistic geometries. In *Proceedings of 30th Conference on Uncertainty in Artificial Intelligence (uai 2014)*. AUAI Press Corvallis, 2014.

30. C. Trapnell, D. Cacchiarelli, J. Grimsby, P. Pokharel, S. Li, M. Morse, N. J. Lennon, K. J. Livak, T. S. Mikkelsen, and J. L. Rinn. The dynamics and regulators of cell fate decisions are revealed by pseudotemporal ordering of single cells. *Nature biotechnology*, 32(4):381–386, 2014.

31. L. Van der Maaten and G. Hinton. Visualizing data using t-SNE. *Journal of Machine Learning Research*, 9(2579-2605):85, 2008.

32. C. Waddington. Principles of development and differentiation, CH Waddington. *Current concepts in biology series.*, 1966.

33. C. H. Waddington. *The strategy of the genes*, volume 20. Routledge, 2014.

34. L. Yan, M. Yang, H. Guo, L. Yang, J. Wu, R. Li, P. Liu, Y. Lian, X. Zheng, J. Yan, et al. Single-cell RNA-Seq profiling of human preimplantation embryos and embryonic stem cells. *Nature structural & molecular biology*, 20(9):1131–1139, 2013.